LA-6633-MS
Informal Report

UC-20 and UC-21

Issued: December 1976

C.3

Sputtering Erosion of Fusion Reactor Cavity Walls

by

I. O. Bohachevsky
J. F. Hafer

los alamos
scientific laboratory
of the University of California
LOS ALAMOS, NEW MEXICO 87545

An Affirmative Action/Equal Opportunity Employer

Printed in the United States of America. Available from
National Technical Information Service
U.S. Department of Commerce
5285 Port Royal Road
Springfield, VA 22161
Price: Printed Copy $4.00 Microfiche $3.00

SPUTTERING EROSION OF FUSION REACTOR CAVITY WALLS

by

I. O. Bohachevsky and J. F. Hafer

ABSTRACT

Devised are functions that describe the
empirically and theoretically determined
behavior of sputtering coefficients. These
functions are used in a computer program that
calculates erosion rates and total erosion of
surfaces bombarded by ion beams of specified
intensity. Presented here are analytic
expressions that describe the effects of ion
energy and angle of incidence, computational
procedures, and results. Results, computed
for alpha, triton, deuteron, and heavy-metal
ions bombarding niobium, carbon, and iron
surfaces indicate that for pellets with heavy
metal shell structures sputtering erosion
should be carefully considered and properly
designed for.

I.   INTRODUCTION

Explosive combustion of a deuterium-tritium fuel pellet in

laser-induced fusion reactors produces primarily high-energy

neutrons and plasma debris. By striking a solid surface the

momentum of these energetic particles is transferred to atoms

surrounding the point of impact. Thus, an atom of the solid near

the surface may acquire sufficient momentum in the perpendicular

direction to break the surface bond and to escape. This phenomenon is known as sputtering; it is described by the sputtering coefficient S, which is numerically equal to the number of surface (or subsurface) atoms that escape per striking ion.

Due to relatively shallow penetration of striking ions, the surface atoms in most cases escape in the direction from which the impinging ions arrive. This mechanism is sometimes called "backward" sputtering. Some impinging particles, however, may have sufficient energy to penetrate the solid and to escape on the opposite side, taking some surrounding atoms along. This phenomenon is termed forward or transmission sputtering; energetic neutrons are one kind of particles precipitating it. In this paper we will limit our discussion and computations to backward sputtering.

Sputtering is encountered in many technologies; e.g., aerospace vehicles may be damaged by sputtering due to impinging interplanetary dust particles, or cathodes are eroded by ions of the electric arc. In controlled thermonuclear-fusion programs sputtering is cause for concern for two reasons. First, in magnetically confined reactors, sputtering may introduce sufficient amounts of impurities into the plasma to inhibit or even prevent efficient burn. Second, in inertially confined reactors, pellet microexplosions generate energetic plasma debris that may cause considerable surface erosion between the explosions.

The formulation, computations, and results reported in this paper have been generated to determine the extent of surface

2

erosion in an inertially confined laser-induced fusion reactor. The particular design for which the results are intended is the magnetically protected wall concept.[1] It has been described previously in Ref. 1; here we briefly mention only its main feature--a cylindrical reaction cavity in which magnetic lines of force parallel to the cylinder axis protect the wall from plasma debris by guiding the particles into energy sinks placed at the ends of the cylinder as shown in Fig. 1. Because plasma debris is composed of fast-traveling light and heavy ions, considerable erosion of energy-sink surfaces may be expected.

In this report we will discuss sputtering in general, introduce analytic expressions for the description of the effects of ion energy and angle of incidence, set up expressions for erosion rate and total erosion of a surface by an ion beam, describe computational procedure, and present the results. Conclusions drawn from these results will also be outlined briefly.

II. SPUTTERING EROSION

A. General Discussion

In sputtering calculations one has to keep in mind the distinction between theoretical definition and experimental determinations of the sputtering coefficient S. As indicated previously, S is defined as the number of solid atoms knocked out of the surface by one striking ion. However, it is not possible

Pellet Injection

Cylindrical Blanket

Solenoid Coils

Bare First Wall

Magnetic Field

Inner Cone

Dry Wall

Conical Energy Sink

Outer Cone

Coolant

Coolant

Partial Vacuum

To Heat Exchanger

To Heat Exchanger

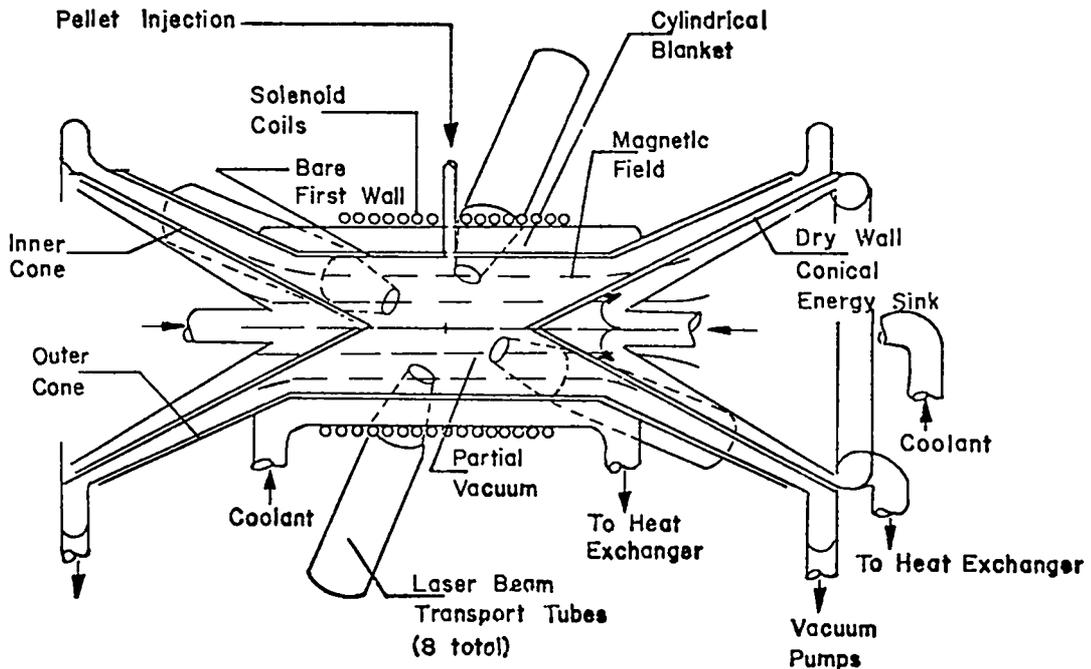Laser Beam Transport Tubes (8 total)

Vacuum Pumps

Fig. 1. Cylindrical reactor cavity with magnetically protected wall and conical energy sinks.

to perform an experiment that would match the above definition; sputtering coefficients are therefore determined by bombarding a surface with a specified ion beam of intensity n ions/s and measuring the amount of sputtered material after a given length of time t. In this process, modification of the surface properties by the implanted ions, redeposition of sputtered ions, and similar factors are not accounted for in the theoretical definition of S. Because the actual environment resembles experimental conditions much closer than the theoretical definition of S, theoretical determinations of sputtering coefficients are of limited value in practical calculations. They should be used only when experimental data are nonexistent or when needed to supplement

inadequate experimental data. We will indicate later how theoretical results are used in our work.

For feasibility studies, preliminary design analyses, and other engineering applications it is more convenient to know surface erosion rather than the sputtering coefficient itself. This quantity is determined by integrating the product of the sputtering coefficient and the ion flux over all energies and angles of incidence to obtain the erosion rate and then integrating the rate with respect to time. It will be convenient to present the relevant expressions after S has been determined and after its dependence on different parameters has been discussed.

B. Empirical Determination of S

The amount of material sputtered from a surface depends, in general, on the mass, charge, energy, and angle of incidence of the striking ions and on target properties, e.g., surface temperature and finish. The dependence on each of these parameters is usually determined by varying them in a series of experiments in which the remaining factors are kept constant.

Effects of surface temperature and roughness have not been investigated systematically. Data on the dependence of sputtering on target temperature appear inconclusive and mostly limited to temperature recording during investigation of other effects.[2,3,4]

The effect of surface deviations from a plane on sputtering yield has been reported in only one reference.[5] In view of this lack of information we assume in our computations that the sputtering coefficient S is independent of both target surface

5

temperature and finish. The following discussion will show that these effects can be incorporated easily into our analysis when adequate and reliable data become available.

Results of sputtering experiments are customarily reported as graphs or tables showing the dependence of sputtering yield on either ion energy or angle of incidence for a given pair of ion and target materials. It is therefore natural to postulate that the sputtering coefficient S will be in the form of a product of two factors: one describing its dependence on ion energy, the other on ion angle of incidence. Accordingly, for a given ion-target combination, we set

$$S(E,\theta) = S_1(E)S_2(\theta) , \qquad (1)$$

where E denotes the energy and θ the angle of ion incidence measured from the normal to the surface.

The dependence of sputtering on the energy of the striking ions is by far the most extensively studied aspect of the phenomenon. The literature is too vast to be discussed here; the data obtained have been summarized and reviewed recently by Carter and Colligan[2] and by Behrisch.[6] The following dependence emerged from the numerous investigations.[2] There is a threshold energy E_0 below which no sputtering occurs; above E_0, S_1 rises gradually, becomes nearly linear with E in a certain range, reaches a maximum, and decreases asymptotically to zero as $\ell nE/E$. This behavior is illustrated schematically in Fig. 2. The above described behavior is physically plausible because E_0 is related to the energy required to break both the bulk and surface bonds
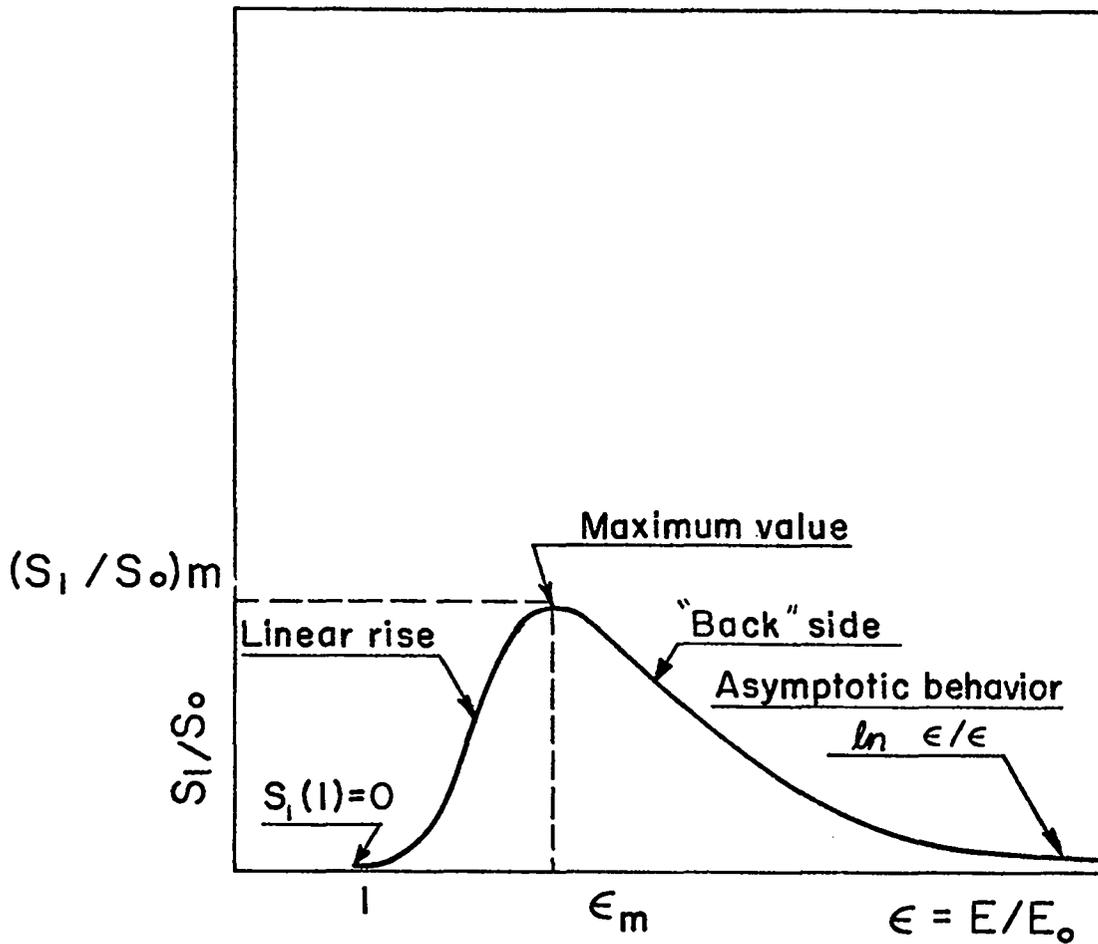
6

Fig. 2. Energy dependence of sputtering yield--schematic.

and because the decrease beyond maximum is due to the increasing depth of penetration of energetic ions, which makes it difficult for the effects to propagate back to the surface before dissipating.

Some reflection will show that the behavior of S_1 depicted in Fig. 2 can be described with the following analytic expression, which possesses the theoretically determined asymptotic behavior at infinity:

$$S_1 \equiv 0, \quad \epsilon \leq 1,$$

$$S_1 = S_0 \frac{(\ell n \varepsilon)^{1+c/\varepsilon}}{\varepsilon^{1+b/\varepsilon}} \quad , \quad \varepsilon \geq 1 \quad , \tag{2}$$

where $\varepsilon = E/E_0$ and S_0, b, and c are positive constants to be determined from empirical data. When sufficient data points are available (more than 5 to 10), the constants S_0, b, and c can be calculated to approximate most of the experimentally determined dependencies to within a few percent; the agreement with particular data points will be demonstrated in Sec. II.D. However, when only a few experimental points are available, the determination of coefficients is not reliable and should be supplemented with physico-theoretical considerations.

The effect of the angle of incidence, θ, on the sputtering coefficient, S_2, has beeen studied by many investigators.[2,6,7,8,9] They found that, in general, the reciprocal of $\cos\theta$ reflects the behavior of $S_2(\theta)$, but, in some cases, a negative exponent different from unity better approximates the data. Clearly, such an increasing behavior can persist only to a maximum value of S_2, which occurs for θ in the neighborhood of $60°$ to $80°$; after the maximum is attained, $S_2(\theta)$ must vanish at $\theta = 90°$ because sputtering cannot be induced by ions travelling parallel to the surface. Thus, $S_2(\theta)$ must start from unity at $\theta = 0$ (by definition) with initially horizontal slope, increase to a maximum somewhere before $\theta = 90°$, and vanish precipitously at $\theta = 90°$. A function with these properties is given by:

$$S_2 = [e^{gx^2}(1 - x^2)]^h \quad , \tag{3}$$

where $x = 2\theta/\pi$ and the parameters g and h specify the location, x_m, and magnitude, S_{2m}, of the maximum value of $S_2(\theta)$. In terms of these quantities g and h are given by:

$$g = \frac{1}{1 - x_m^2}$$

$$h = \frac{\ln S_{2m}}{gx_m^2 + \ln(1 - x_m^2)} \quad . \tag{4}$$

For specific computations the values of x_m and S_{2m} are chosen on the basis of experimental data. The angular dependence $S_2(\theta)$ given by Eq. (3) is shown in Fig. 3 for $S_{2m} = 2.5$ at $\theta_m = 75^\circ$ together with experimental data from Ref. 9 and the reciprocal cosine relation; the agreement appears satisfactory.

C. Erosion Rate and Erosion

As indicated previously, for applications in the analysis of the magnetically protected laser-induced fusion-reactor concept it is necessary to know the surface erosion rate and the total erosion after some specified length of time. With $S(E,\theta)$, given by Eqs. (1), (2), and (3), the erosion rate Err is given by:

$$Err = \frac{a}{A\rho} \iint S(E,\theta)n(E,\theta,t)dEd\theta \quad , \tag{5}$$

where a is the atomic weight, A is Avogadro's number, and ρ is the density of the target material. The factor $a/A\rho$ converts the units of erosion rate, Err, from atoms/s to cm^3/s which are more appropriate for engineering analyses. In some parametric studies it is convenient to interpret the quantity $n(E,\theta,t)$ as ion flux
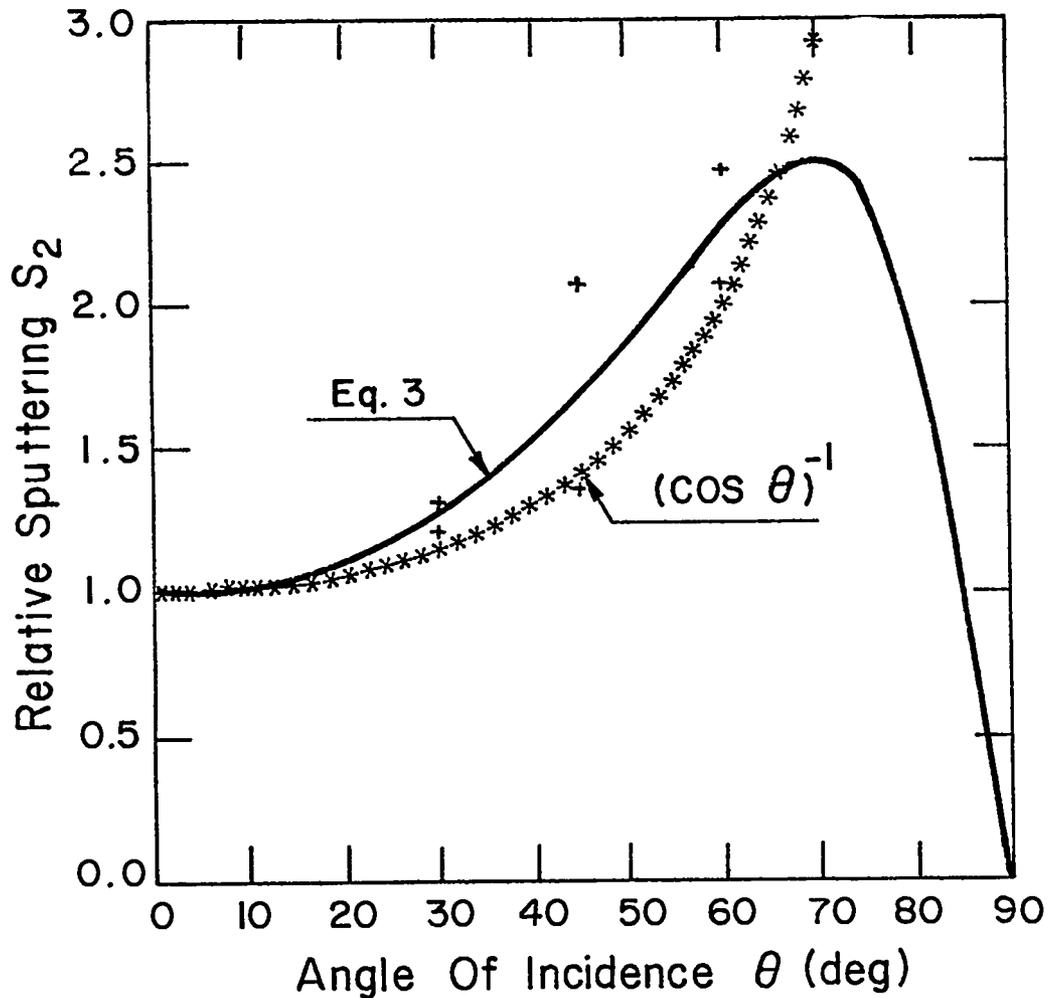
9

Fig. 3. Dependence of sputtering yield on angle of incidence.

per unit area (ions/s·cm^2) so that the units of the erosion rate

are cm/s and Err is a direct indication of the rate at which the

surface recedes due to sputtering.

The total erosion after any given length of time τ is given

by:

$$Er = \int_0^\tau Err(t)dt \ .$$ (6)

D. Validity of the Model

As indicated previously, Eqs. (2) and (3), which constitute

our sputtering model, describe the correct qualitative variation

10

of sputtering yield with ion energy and angle of incidence. In the following discussion we will demonstrate the quantitative agreement of these expressions with theoretical and experimental results.

Before proceeding with specific comparisons we note that one theoretical result, namely the asymptotic behavior of sputtering at large energies, is included in the model, because of the form of Eq. (2). This asymptotic behavior has been theoretically determined[2,10,11,12] to be $\ln \varepsilon / \varepsilon$ and it is the limiting form of Eq. (2) as $\varepsilon \to \infty$. In addition, $S_1(E)$ given by Eq. (2) (with $b > 0$, $c > 0$) has vanishing slope at the threshold energy $\varepsilon = 1$, and for $\varepsilon \to \infty$, as the experimental evidence appears to suggest.

Figure 4 shows $S_1(E)$ for the bombardment of niobium with alpha particles given by Eq. (2) in which the constants S_o, b, and c have been determined with a least-square regression to experimental data (indicated by crosses) reported by Rosenberg and Wehner,[5] Carter and Colligan,[2] Yonts,[4] Summers et al.,[9] and Kaminsky.[13] The agreement appears to be everywhere within experimental error. The dashed curve in Fig. 4 plots the theoretical dependence derived by Goldman and Simon[10] based on the assumption of Rutherford scattering cross-sections, which is a good approximation at high energies. The two curves are identical in the range where the Goldman and Simon theory is valid; this agreement is real because the Goldman-Simon expression for sputtering has no adjustable parameters.

The maximum sputtering yield indicated by Eq. (2) is 0.12 atoms/ion at $\sim$ 4750 eV; theoretical modeling of the sputtering phenomenon[11,12] indicates a maximum of 0.237 atoms/ion at 3864 eV.
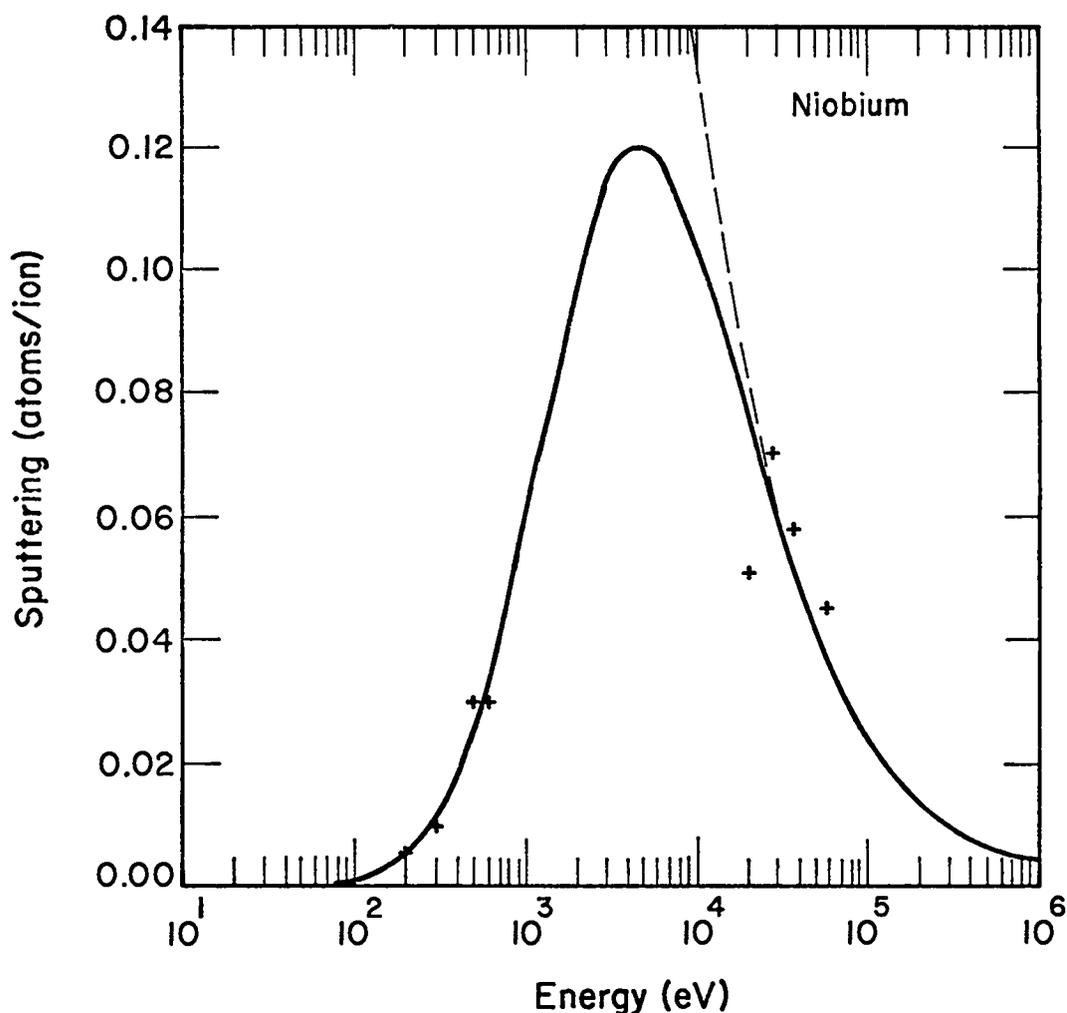
Fig. 4.   Sputtering yield of niobium bombarded with α particles.

Such correspondence is reasonable in view of the discrepancy between theoretical definition and experimental determinations of sputtering mentioned earlier.

Figures 5 and 6 show sputtering yield for iron and carbon bombarded with alpha particles predicted by Eq. (2) with coefficients determined from experimental results (indicated by crosses) reported by Rosenberg and Wehner,[5] Carter and Colligan,[2] and Kulcinski et al.[14] Again the agreement is excellent.
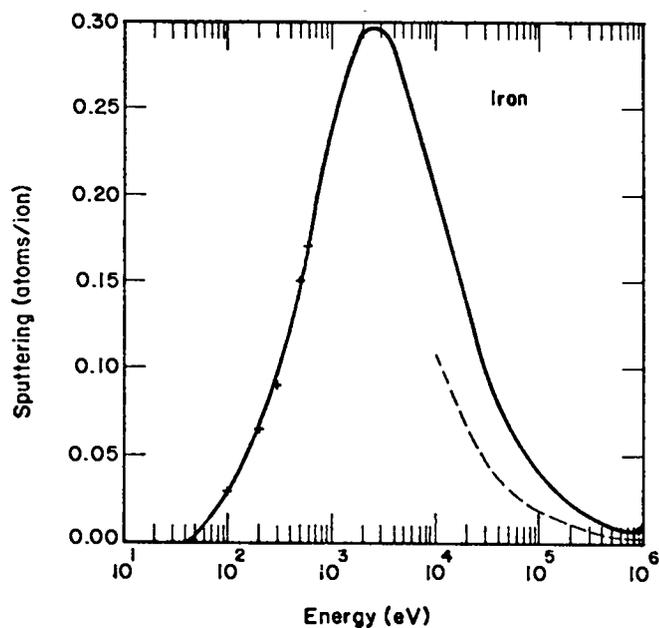
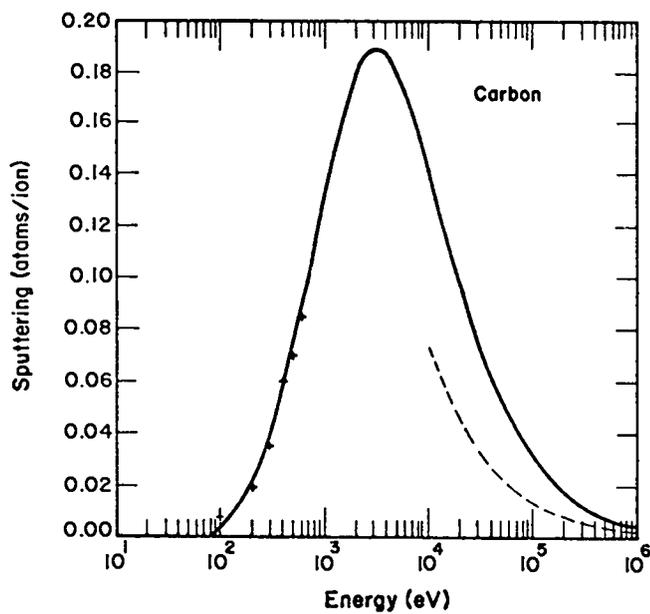Fig. 5. Sputtering yield of iron bombarded with α particles.

Fig. 6. Sputtering yield of carbon bombarded with α particles.

13

However, the agreement with asymptotic behavior predicted by the analysis of Goldman and Simon,[10] is not as good as in the case of niobium; this may be caused by the fact that for iron and carbon we had no data points for the high-energy "back" of the sputtering curve.

Expression (2) predicts a maximum sputtering of almost 0.30 atoms/ion at 3000 eV for iron and of 0.19 atoms/ion at 3000 eV for carbon; the theoretical analyses of Sigmund[11] and Koichi Kanaya et al.[12] predict a maximum of 0.482 atoms/ion at 2207 eV for iron and 0.129 atoms/ion at 514 eV for carbon. In addition to the previously mentioned difference between theoretical and experimental sputtering, there are, for carbon, uncertainties about the type of carbon used in different experiments and about its lattice orientation (if lattices existed) during ion bombardment; therefore, the comparison of theory and experiment for this material is not very meaningful.

The three calculations, above, show that Eq. (2) approximates experimental data over the entire range of energy values with satisfactory accuracy. Before concluding this discussion of the validity of the proposed approximation we indicate briefly how Eq. (2) may be used in conjunction with theory when the data are insufficient to determine all three constants; additional details will be given in the next section when computational proocedures are described. In the case of insufficient data we begin with a set of values for S_o, b, and c obtained for some similar ion-target pair and vary them until the curve approximates the available data and its maximum occurs sufficiently near the

14

theoretically predicted location of the maximum (locations of theoretically and experimentally determined sputtering maxima, in general, agree much better than the amplitudes of the maxima). In this way the ability to change the approximation and determination of its acceptability are left to the user. The above procedure should be used also when Eq. (2) has multiple maxima with regressively determined coefficients; this phenomenon is very rare, but we were unable to exclude ranges of coefficients analytically where it occurs.

The approximation, by Eq. (3), of the angular dependence of sputtering has been compared in Sec. II.B. (Fig. 3) with experimental data and with the usually postulated reciprocal cosine relation; agreement was satisfactory. In view of the scarcity of empirical and theoretical results, this topic will not be discussed further.

III. COMPUTATIONS

Computation of the sputtering erosion rate, Err, with Eqs. (1) and (5) was programmed in a modular form to facilitate parametric studies and calculations of the erosion of reactor cavity components. The different modules or subroutines of the main program determine different factors appearing in Eq. (5).

A.   Sputtering Coefficient $S(E, \theta)$

The dependence of the sputtering coefficient on ion energy, $S_1(E)$, given by Eq. (2) is determined in a routine that has two options: In one, the constants S_0, b, and c are calculated to

obtain a least-square approximation to given empirical data; in the second, the user may interact with the computer to change these constants in such a way as to obtain, in his judgment, a better agreement with the theoretically determined location and/or magnitude of the peak of the sputtering curve. The latter procedure was mentioned in Sec. II.D. The results of Goldman and Simon,[10] Sigmund,[11] or Koichi Kanaya et al.[12] may be used for this purpose.

The dependence of the sputtering coefficient on ion angle of incidence, $S_2(\theta)$, given by Eq. (3), may be determined also in two ways. Either the constants g and h are calculated from Eq. (4) and from direct specification of the parameters x_m and S_{2m}, as indicated previously, or g and h are determined from a least-squares approximation to available data.

B.   Ion Flux n(E,θ,t)

The present sputtering computer program has two options for the specification of the ion flux $n(E,\theta,t)$: for parametric studies it is convenient to specify a time-independent flux intensity in the form $n_1(E)n_2(\theta)$, and for the determination of the erosion of reactor components it is necessary to use ion fluxes obtained from realistic plasma expansion computations.

To investigate the effects of ion energy, the flux $n_1(E)$ may be specified either as a constant n_o or as a Maxwellian distribution given by:

$$n_1(E) = 2n_o(2E_m)^{-3/2} \sqrt{E/\pi}\ e^{-E/2E_m} \tag{7}$$

16

where E_m denotes the location of the maximum intensity. Equation (7) is to be used only in the interval between the threshold energy E_0 and some high cutoff value (typically, 10 MeV), which must be finite for numerical evaluation of the integral in Eq. (5).

In investigating the effects of the ion angle of incidence, we provide, for reasons of convenience, two options for defining the factor $n_2(\theta)$: (1) make $n_2(\theta)$ constant (namely unity), i.e., postulate that all ions are incident at the same angle; (2) assume that the angle of incidence θ is distributed like cosine in the interval $0 \leq \theta \leq \pi/2$, i.e.,

$$n_2(\theta) = \frac{\cos(\theta - \theta_p)}{\cos\theta_p + \sin\theta_p} \quad , \tag{8}$$

where θ_p is the location of the maximum intensity (also in the interval $0 < \theta_p < \pi/2$), and the denominator is the normalizing factor that makes $n_2(\theta)$ a probability distribution. Because the factor n_0 was included with the energy dependence $n_1(E)$, it is not required here.

For the sputtering-erosion calculations of reactor cavity components the ion flux $n(E,\theta,t)$ is obtained from computer simulation of plasma expansion following fuel-pellet microexplosion. The code used for this purpose (LIFE--Laser Induced Fusion Explosion) is based on the approach described by Dickman et al.[15] and generalized to include a large number (50) of different ions. It determines the trajectory of each ion after the microexplosion and records, on a magnetic tape, the location, time, energy, and angle of incidence for every ion colliding with

a wall. This tape is read by the sputtering code and the information is processed to obtain $n(E, \theta, t)$.

C.   Erosion Rate and Total Erosion

When ion and target materials are selected and the factors S_1, S_2, n_1, and n_2 are determined with appropriate procedures as discussed above, Eqs. (5) and (6) are evaluated in a standard way to yield erosion rate and total erosion of the given surface; the results will be presented and discussed in the next section. When output of plasma-expansion computations is used to obtain the ion flux, it is more convenient to circumvent the determination of erosion rate and to calculate the total erosion per pulse (microexplosion) directly by summing over all particles impinging onto the boundary; our results will be presented in this form.

IV.   CALCULATIONS AND RESULTS

Parametric studies and erosion calculations of reactor cavity components have been performed for several types of ions, alphas, tritons, deuterons, and heavy metals incident on three materials: niobium, carbon, and iron. Some sputtering data used in these studies are presented in Figs. 3 through 6. Because we were unable to locate sputtering data for tritium ions we obtained the tritium sputtering curve (for a niobium target) from the alpha curve. To do it, we adjusted the coefficients of alpha and deuteron data to place the maximum near the theoretically predicted maximum for tritium ions and to make its magnitude
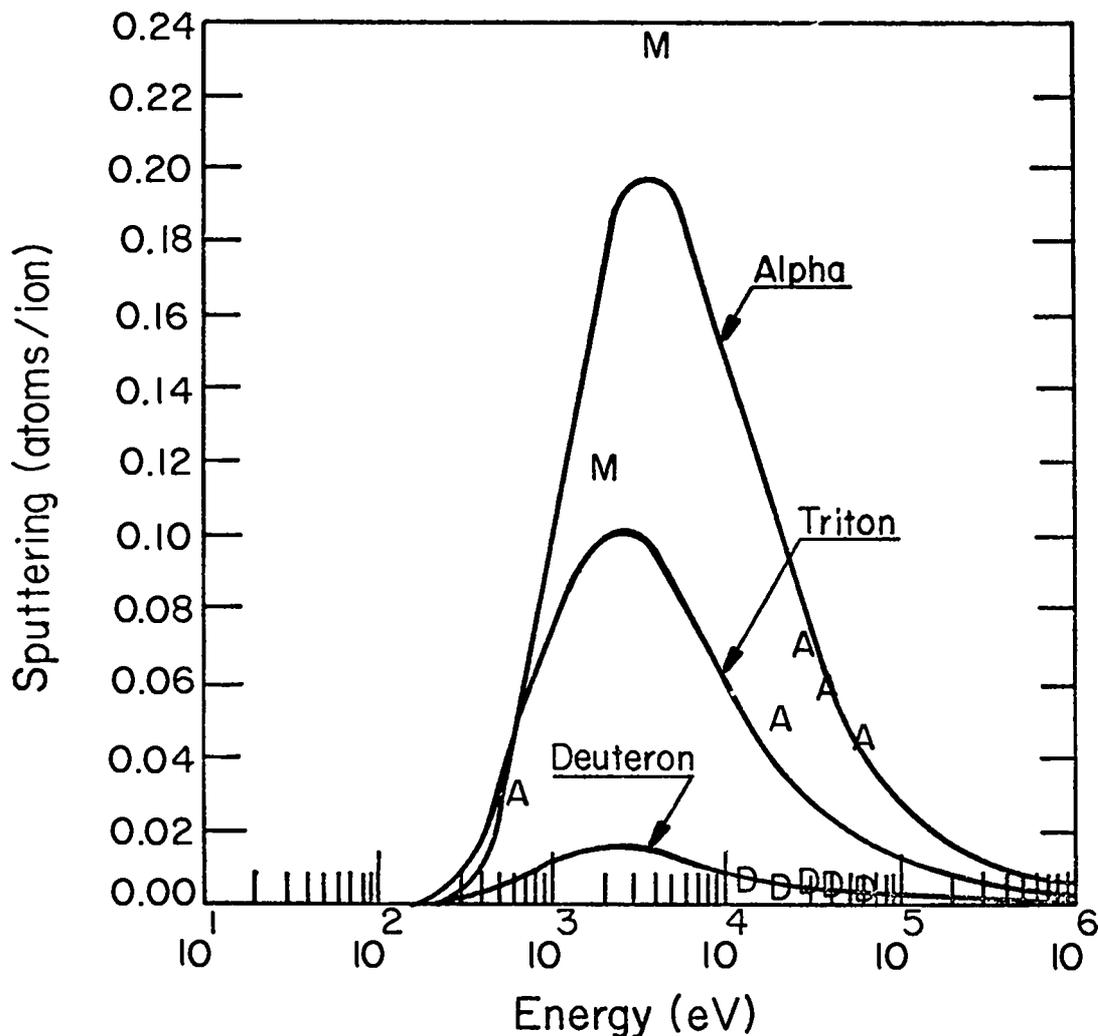
Fig. 7. Sputtering yield of niobium bombarded with α, T^+ and D^+ ions.

approximately equal to the average of the alpha and deuteron maxima; the result is shown in Fig. 7.

A.   Parametric Studies

Calculations were performed to show the effects of ion energy and angle of incidence for an ion beam of peak intensity 8×10^{13} alpha particles per square centimeter per second; this is an average representative flux intensity that must be absorbed by the energy sinks in a magnetically protected reactor cavity operating at one pulse per second.

Shown in Fig. 8 is the erosion rate as a function of peak energy for an ion beam with Maxwellian energy distribution incident normally on iron, niobium, and carbon targets. In the range of energies included in the graph, the erosion rate decreases rapidly with increasing energy because this energy range is on the "back" side of the sputtering curve (see Fig. 2). the value of a typical erosion rate, 2×10^{-11} cm/s, is equivalent to $\sim 6.5 \times 10^{-3}$ mm/yr and shows that this phenomenon will not be a critical design criterion even at 10 pps.

The effect of the angle of incidence on the erosion rate of different materials bombarded with beams of different energy is shown in Fig. 9. In the range of angles from 0° to 75° the variation is small, not exceeding 25%. In these calculations the sputtering coefficient S_2 had a maximum of 2.5 located at 75°. Thus it appears that in preliminary analyses of reactor cavity configurations the effects of the angle of incidence need not be considered.

B. Erosion of Reactor Cavity Wall

As mentioned previously, plasma expansion computations are used to determine ion fluxes that erode internal surfaces of fusion reactors. Typical results are illustrated in Figs.10 and 11. Shown in Fig. 10 is the flux intensity integrated over the pulse duration incident on the conical energy-sink surface as a function of axial position. The ions are concentrated near the axis, and it is very difficult to shape the magnetic field in such a way as to guide them further down the cone and simultaneously to continue protecting the upper cylindrical surface from plasma
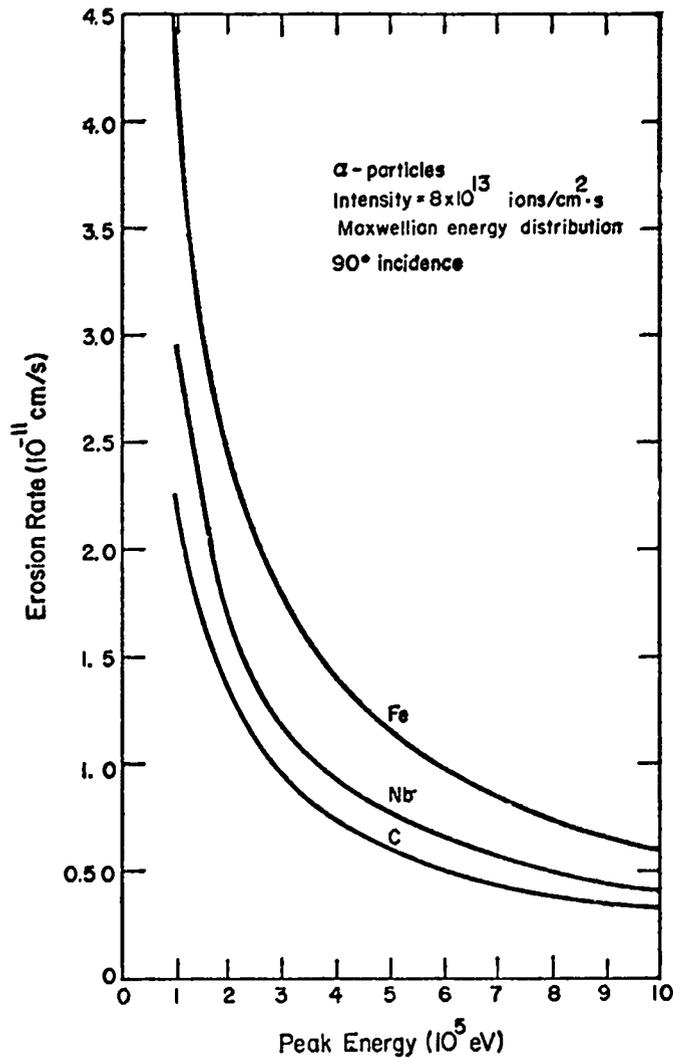
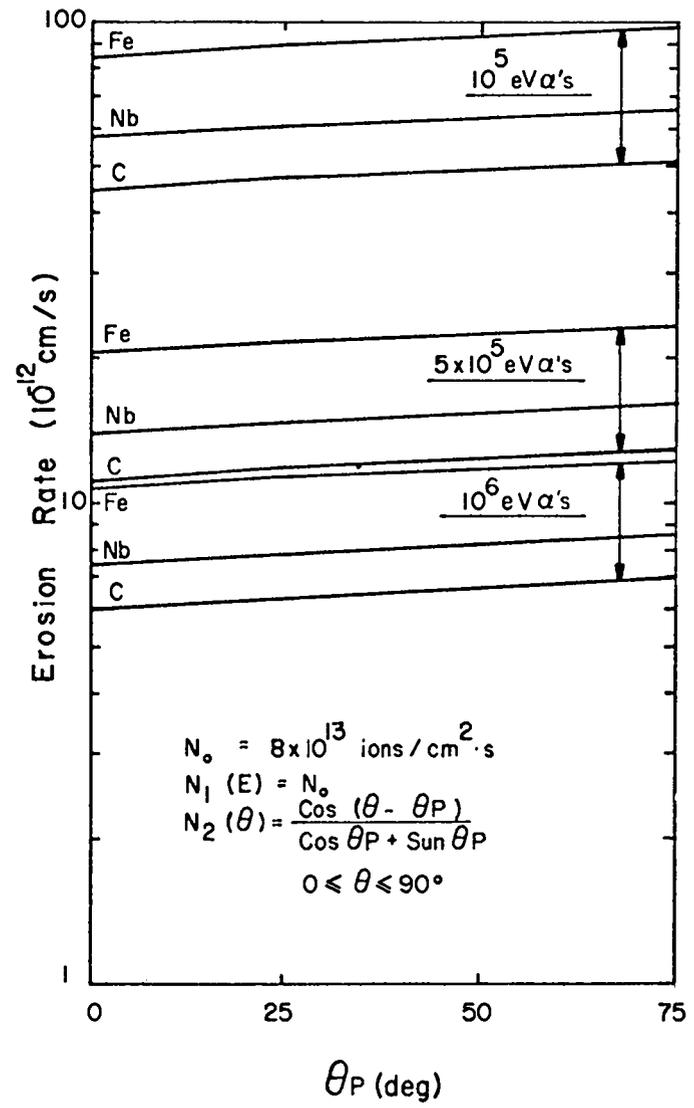Fig. 8. Energy dependence of erosion rate.

Fig. 9. Angle-of-incidence dependence of erosion rate.
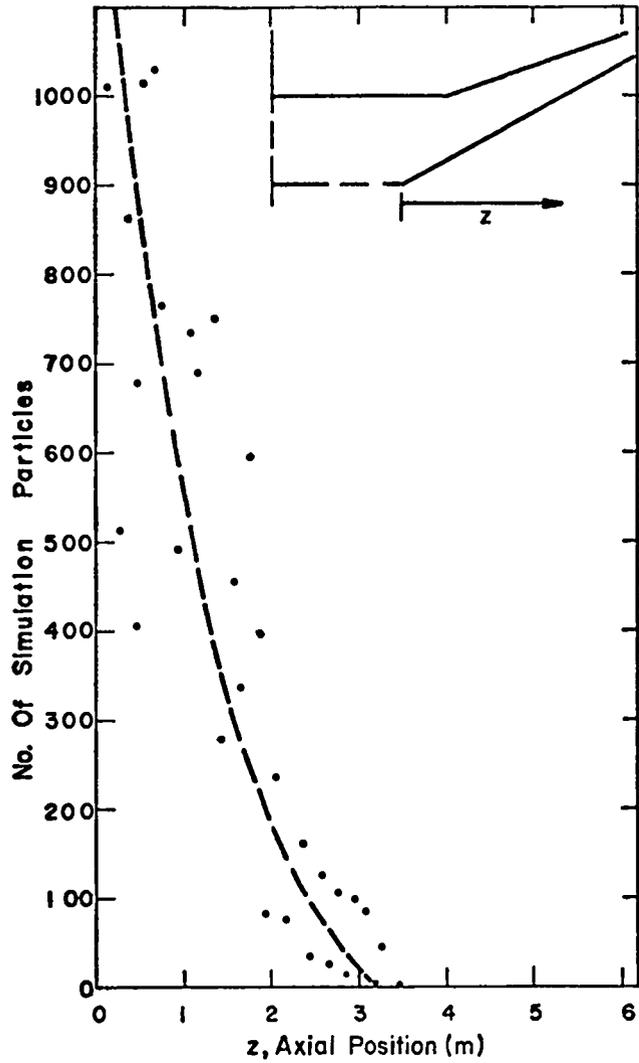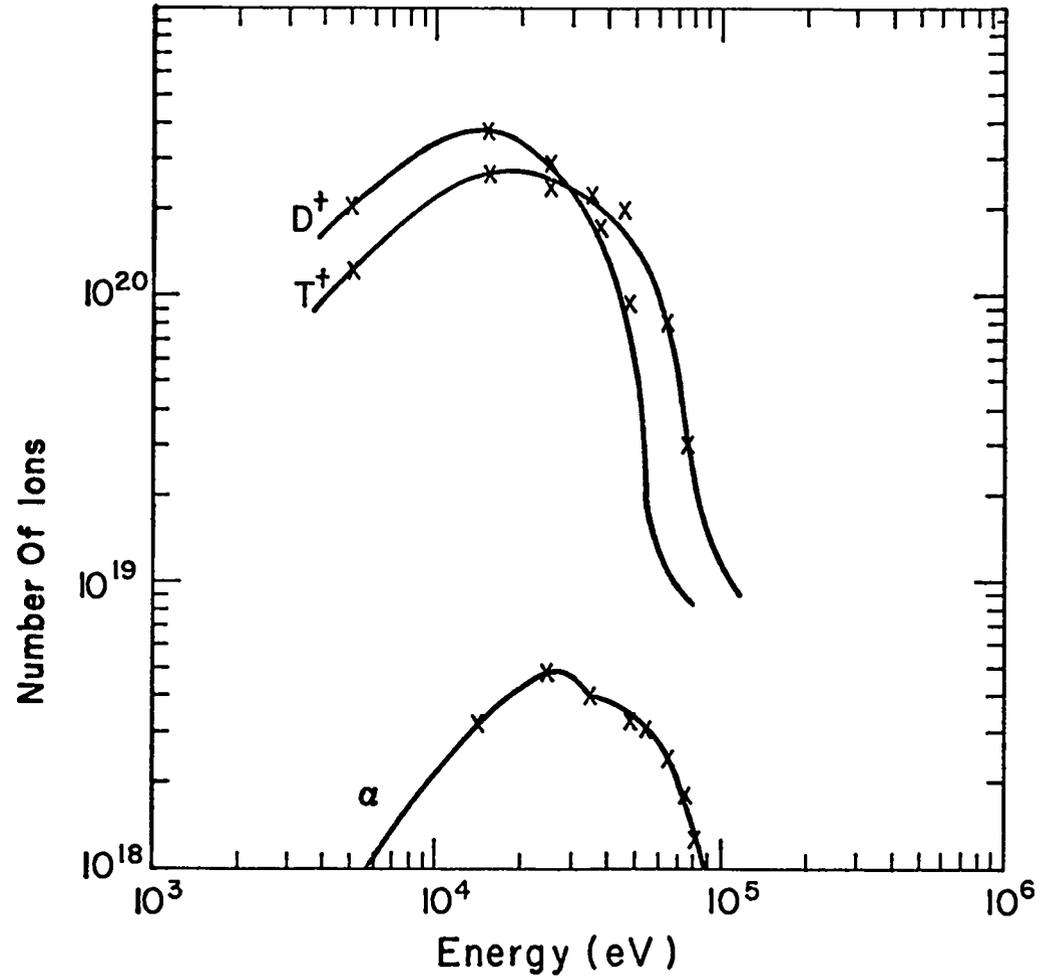
Fig. 10. Ion flux at energy sink surface.

Fig. 11. Ion energy distribution from a "LIFE" code computation for a 100-MJ-yield bare DT pellet.

debris. The energy distribution of the three types of ions--alphas, tritons, and deuterons--produced in a bare-pellet microexplosion are shown in Fig. 11.

By combining above results with those shown in Figs. 7 and 3 we calculate the sputtering erosion with Eq. (5) and (6); the result is shown in Fig. 12. The erosion near the cone vertex is excessive ($\sim$ 3 cm/yr at 1 pps) and about 30 times greater than the average that would be obtained if the ions were uniformly distributed over the energy sink surface.

This unfavorable situation can be alleviated by changing the geometry of the reactor cavity so that: (a) the magnetic lines diverge towards the end where the energy sink is located and (b) the most vulnerable point on the axis of symmetry is moved further away from the microexplosion so that the ions have more time to diffuse across the lines of force before striking the energy sink. Shown in Fig. 13 is the modified configuration with cone half-angle θ_c = 90° and the corresponding erosion for fields of 1000 and 2000 G. The sputtering erosion is reduced significantly, however it is still large near the axis of symmetry, and the outer 25% of the energy-sink surface is not utilized efficiently. The distribution of the erosion for the 1000-G field is much more uniform than for 2000 G and the average is lower because the 1000-G field was too weak to protect the upper cylindrical wall; consequently $\sim$ 16% of the ions reached the cylinder causing local erosion of $\sim 10^{-9}$ cm/pulse.

The performance of the energy sink is further improved by increasing the cone half-angle beyond 90° resulting in a
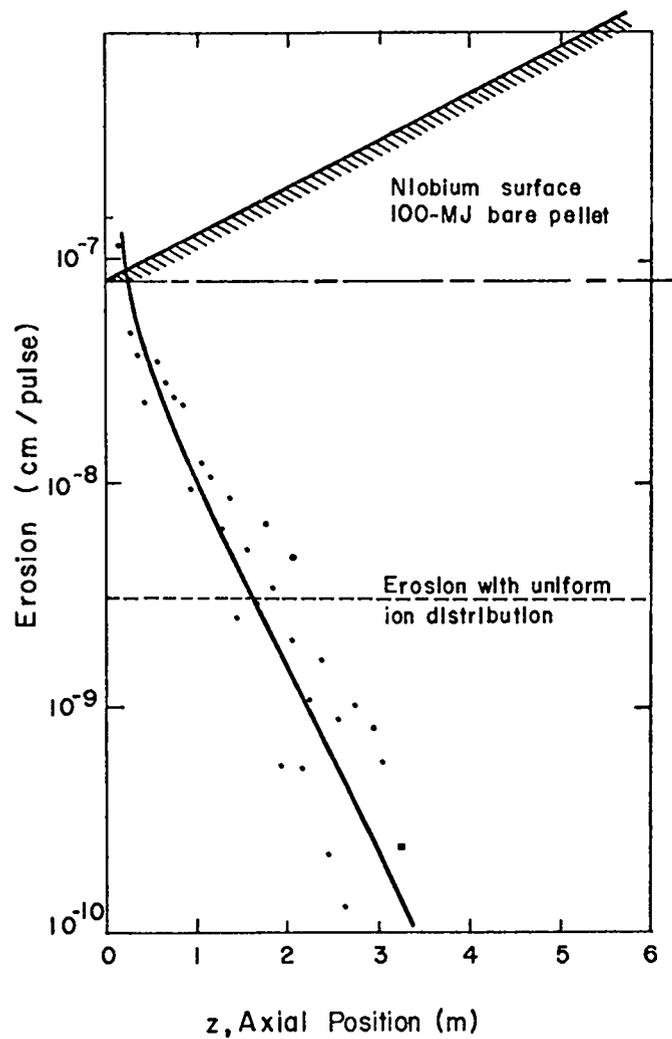
Fig. 12.   Erosion of inward-pointing
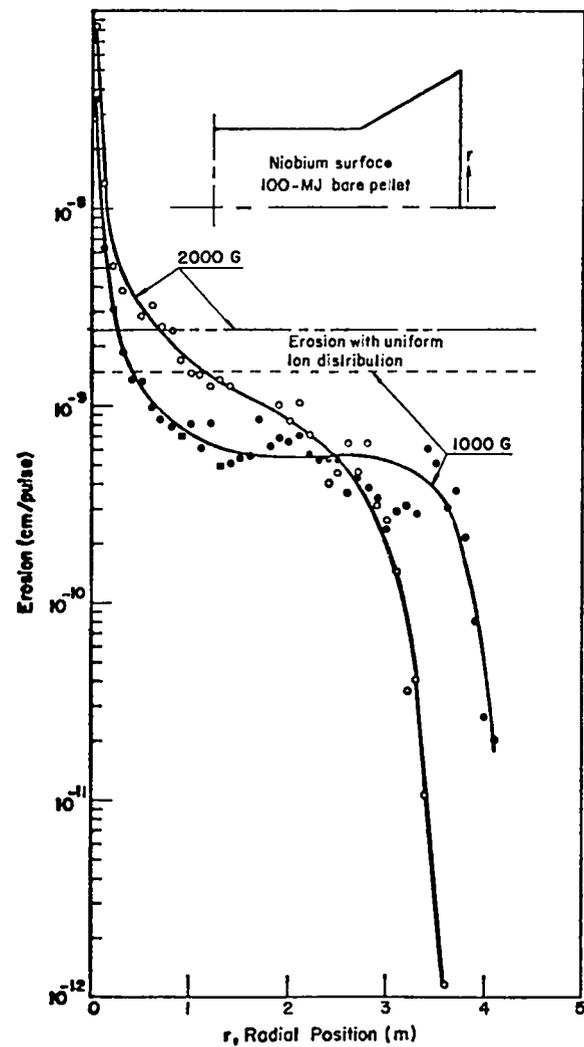conical energy-sink sur-
face.

Fig. 13.   Sputtering erosion of
flat plate energy-sink
surface.

configuration shown in the upper part of Fig. 14. Such "inversion" of the original conical energy sink places the vertex along the axis furthest from the microexplosion while retaining a surface area larger than that of a flat plate shown in Fig. 13. The increased radius in front of the energy sink allows divergence of the magnetic lines.

Unlike preceeding results, the erosion of the outward-pointing conical energy sink was calculated for a pellet with low yield-to-mass ratio (23 MJ yield and a heavy shell).

Because sputtering data for heavy metal ions used in this calculation were not available, Sigmund's theory[11] was employed to determine the sputtering yield $S_1(E)$. The result plotted in Fig. 14 shows that the peak at the center line has been reduced, the erosion is fairly uniform, and its magnitude not excessive ($\sim$ 6 mm/yr average at 1 Hz) even though the sputtering coefficient for the heavy ions is at least 100 times greater than for light ions used to obtain previous results.

V.   SUMMARIZING REMARKS

Present knowledge of sputtering phenomena has been applied to devise a computational procedure for the analysis of sputtering erosion on components of laser-initiated fusion-reactors. Functions have been constructed that analytically approximate empirical and theoretical sputtering-yield data. The procedure has been automated in a computer program that calculates surface erosion rate and total erosion from sputtering-yield data and ion-flux characteristics.
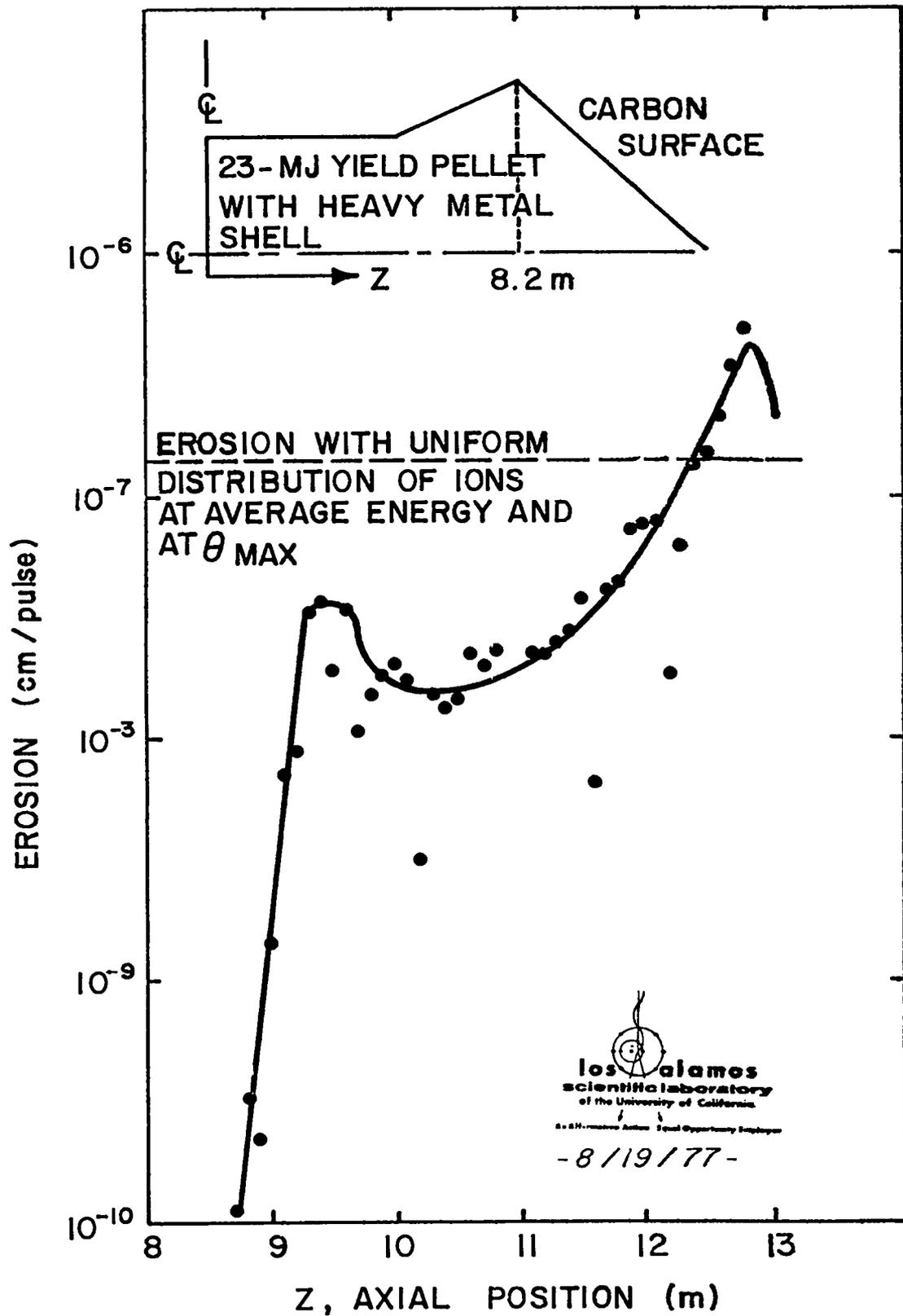
Fig. 14.   Erosion of outward-pointing conical energy-sink surface.

The coded program is used in parametric studies for different ion-beam characteristics and target materials, and to determine the surface erosion of energy sinks in the conceptual design of laser-initiated fusion reactors with magnetically protected cavity walls.

Results thus far indicate that for bare DT fuel pellets that produce only light ions, sputtering erosion will not be a limiting design criterion. This observation is corroborated by the fact that fusion-generated light ions are found mostly in the high-energy tail of the sputtering curve where the yield is low. However, structured pellets produce heavy metal ions, which can cause considerable erosion that will have to be considered carefully in any design.

Further work should include more extensive, realistic, sputtering-erosion calculations; efforts to obtain better sputtering-yield data; and investigations of the dependence of the sputtering coefficient $S_1(E)$ given by Eq. (2) on the parameters that specify its behavior.

ACKNOWLEDGMENT

REFERENCES

1. T. Frank, D. Freiwald, T. Merson, and J. Devaney, "A Laser Fusion Reactor Concept Utilizing Magnetic Fields for Cavity Wall Protection," Proc. of 1st Topical Meeting on the Technology of Controlled Nuclear Fusion, V. I, San Diego, CA, (1974), 83.

2. G. Carter and J. S. Colligan, "Ion Bombardment of Solids," Sputtering, (Elsevier, NY, 1968), Chap. 7, 310-353.

3. T. S. Baer and J. N. Anno, "Fast-Neutron Sputtering of Iron at Various Temperatures," J. Nucl. Mat. $\underline{54}$, 79-84 (1974).

4. O. C. Yonts, "Sputtering of Niobium by D^+ and He^+ Ions," Oak Ridge National Laboratory report ORNL-TM-2692 (September 1969).

5. D. Rosenberg and C. K. Wehner, "Sputtering Yields for Low Energy $He^\pm$, $Kr^\pm$, and $Xe^\pm$ Ion Bombardment," J. Appl. Phys. $\underline{33}$, 1842 (May 1962).

6. R. Behrisch, "First Wall Erosion in Fusion Reactors," Nucl. Fus. $\underline{112}$, 695 (1972).

7. D. J. Barber, F. C. Frank, M. Moss, and J. W. Steeds, "Prediction of Ion Bombardment Surface Topographies Using Frank's Kinematic Theory of Crystal Dissolution," J. Mat. Sci. $\underline{8}$, 1030-1040 (1973).

8. R. P. Edvin, "Measurement of the Sputter Rate of Fused Silica Bombarded by Argon Ions of Energy 12-32 keV," J. Phys., Appl. Phys. $\underline{6}$, 833-841 (1973).

9. A. J. Summers, N. J. Freeman, and N. R. Daly, "Sputtering of Niobum by Niobium, Hydrogen, Deuterium, and Helium Ions in the 10-80 keV Range," J. Appl. Phys. $\underline{42}$, 4774-4778 (1971).

10. D. T. Goldman and A. Simon, "Theory of Sputtering by High Speed Ions," Phys. Rev. $\underline{111}$, 383-386 (July 1958).

11. P. Sigmund, "Theory of Sputtering. I. Sputtering Yield of Amorphous and Polycrystalline Targets," Phys. Rev. $\underline{184}$, 383-416 (August 1969).

12. Koichi Kanaya, Kiichi Hojou, Kikuo Koga, and Kazuyuki Toki, "Consistent Theory of Sputtering of Solid Targets by Ion Bombardment Using Power Potential Law," Jap. J. Appl. Phys. $\underline{12}$, 1297-1206 (September 1963).

13. M. Kaminsky, "Plasma Contamination and Wall Erosion in Thermonuclear Reactors," IEEE Trans. Nucl. Sci. NS$\underline{18}$, 208-217 (1971).

28

14. G. L. Kulcinski, R. W. Conn, G. Lang, L. Wittenberg, D. Sze, J. Kesner, and D. L. Kummer, "A Method to Reduce the Effects of Plasma Contamination and First Wall Erosion in Fusion Reactors," Nucl. Eng. Dept., Univ. of Wisconsin report UWFDM-108 (August 9, 1974, Revised September 15, 1974).

15. D. O. Dickman, R. L. Morse, and C. W. Nielson, "Numerical Simulation of Axisymmetric, Collisionless, Finite-β Plasma," Phys. Fluids $\underline{12}$, 1708-1716.